First-Principle Calculations of the Fundamental Properties of Zno Binary Compound

Abdelghani Lakel[1] , Yousra Megdoud[2,3], Hanane Meddas[1], Yamina Benkrima[4] and Redha Meneceur[5]

[1] Laboratory of Metallic and Semiconducting, Materials, University of Biskra, BP 145 RP, 07000,Biskra, Algeria

[2] Institute of Sciences,University Center of Tipaza, Morsli Abdallah, Algeria.

[3] LPR Laboratory, Département of Physics, Faculty of Science, Badji –Annaba-Address, Algeria.

[4] Ecole NormaleSuperieure de Ouargla, 30000 Ouargla, Algeria,

[5] Unit for the Development of Renewable Energies in Arid Zones (UDERZA), El Oued University, Algeria.

Corresponding author e-mail: a.lakel@univ-biskra.dz

Received 02 September 2023, Accepted 05 January 2024, Published 22 January 2024

Abstract

The oxide zinc (ZnO) nanostructure are studied by the first-principle computational within the framework of the density functional theory (DFT). We studied the structural and electronic for the three phases: wurtzite (B4), zincblende (B3) and rocksalt (B1) of ZnO compound have been reported using the full-potential linearized-augmented plane-wave (FP-LAPW) method is applied to solve the Kohn-Sham equations. We employed both the local-density approximation (LDA) and the generalized-gradient approximation (GGA), which is based on exchange–correlation energy optimization to calculate the total energy. Also, we have used the Engel Vosko-GGA formalism, which optimizes the corresponding potential for band-structure calculations. The calculated lattice parameters and internal coordinates are in very good agreement with the experimental findings. The band structure and Density of States (DOS) diagrams are plotted from the calculated equilibrium lattice parameters. A comparison with the previous studies has been made.

Keywords: ZnO, DFT, LDA, FP-LAPW, Optical Properties. And Density of States (DOS).

***Tob Regul Sci.™ 2024;10(1):*191-206**
DOI: doi.org/10.18001/TRS.10.1.14

Introduction

9To date, several reviews and research papers have been published on the photocatalytic application of ZnO nanostructures ,and all corroborate the fact that, as regards the photocatalytic decomposition of organic pollutants, ZnO is preferred overTiO2 due to features such as its high quantum efficiency, chemical stability, environmental friendliness, simple and cost-effective synthesis process, ability to form any morphology, simple bandgap energy tuning, and ability to

form defect levels in the bandgap space so as to catch visible photons.[1–4]. In addition, several works and reviews have reported that the most important factors for the enhancement of photocatalytic performance of ZnO nanostructures are particle size and oxygen vacancies.[5–10] However, the photocatalytic performance of ZnO is usually enhanced by using doping materials that narrow the bandgap or create several defect energy levels in the bandgap space of ZnO.[4] Of the various doping materials that have been applied, magnesium is the best for ZnO structures because of its ionic radius, which is similar to the ionic radius of zinc. However, MgO with a cubic phase has a high lattice mismatch with the hexagonal phase of ZnO. Indeed, it is employed as one of the best materials to widen the bandgap of ZnO.[11] Although a wide bandgap is a drawback for a photocatalytic material, Mg-doped ZnO nanostructures are, more often than not, used as photocatalysts in abundance.[12–19] Several groups have justified that because the MgdopedZnO bandgap is wider than ZnO bandgap, the former is able to catch more fractions of the solar spectrum than the latter. Etacheri et al. reported that the increase in the bandgap values of ZnO due to Mg2+ resulted in superior textural properties and efficient electron–hole separation, which influenced the enhanced sunlight-driven photocatalytic activity of MgdopedZnO.[12] By using DFT methods, Qiu et al. observed that replacement of Zn2+ ions with Mg2+ ions in the wurtzite ZnO structure largely affected the conduction band (CB), yet left the valence band (VB) of ZnO nearly unchanged.They further reported that the contribution of the Mg 3s orbitals to the CB became more pronounced with an increase in the Mg content, which explained the enhanced photocatalytic activity.[20] They concluded that Mg augments bandgap values and results in superior textural properties and efficient electron–hole separation, all of which ameliorate the sunlight-driven photocatalytic activity of Mg-doped ZnO. Such experimental and theoretical studies, although informative and compelling, were not able to posit a primary factor that improved Mg-doped ZnO photocatalytic performance relative to other doped ZnO nanostructures. To increase the photocatalytic activity of ZnO nanostructures, it has recently become common to employ graphene as an additive in addition to Mg, which does not result in any secondary pollution. In fact, graphene, as an acceptor, augments the electron–hole pair lifetime, which is the most important factor in the photocatalytic activity of a semiconductor. This might explain why graphene has been used more than any other material in hundreds of research articles on the photocatalyst properties of ZnO/graphene nanocomposites.[1, 2, 21, 22] Several works have also reported studies of Mg-doped ZnO/reduced graphene oxide (rGO) nanocomposites, in which it was observed that Mg and graphene significantly enhanced the photocatalytic performance of ZnO.[14, 23, 24] However, no exact claim can be found in these papers as to the roles of Mg and graphene in such photocatalytic activity. The concept of doping impurity atoms in ZnO, has added several new dimension to its versatile applications. Consequently, the contaminated ZnO has accomplished extrinsic features, such as electro-optic [1], magnetic [2-3], magneto-optic [4], electromagnetic [5] and piezoelectric [6] in addition to its fascinating electronic and magnetic properties. Thus it has found numerous applications in several novel fields including optoelectronic and spintronics.

However the nature of the newly developed features is strongly dependent on dopant materials. For instance, the energy gap of ZnO can be engineered to a value appropriate for optoelectronic applications by doping elements like Al [7-8], Ga [7, 9], or In [10-11] etc. ZnO doped with such elements is potential material for the fabrication of transparent conducting oxides (TCOs) and is considered as an alternative costly Indium-Tin-Oxide (ITO). The structure of this paper is delineated as follows: 'Section 2' expounds upon the ZnO Binary compounds, elucidated via the utilization of the Wien2K code, rooted in the density functional theory (DFT). The ensuing 'Section 3' derives implications for the utilization of these materials within the realm of photovoltaic applications, predicated upon the results gleaned. Finally, 'Section 4' culminates in a comprehensive summary of the paper's conclusions, accompanied by the listing of the corresponding author.

2. Details of Calculations:

We apply the most recently developed Vienna package WIEN2k[25,26] for the full-potential augmented plane-waves plus local orbitals (FP-APW) method within the density functional theory (DFT) [27,é_], for which the electron exchange correlation energy, is described in the generalized gradient approximation (GGA) using the Perdew–Burke– Enzerhof functional parameterization [29]. The APW +lo method expands the Kohn–Sham orbitals in atomic like orbitals inside the atomic muffin-tin (MT) spheres and plane waves in the interstitial region. The details of the method have been described in the literature [30–31]. Basis functions, electron densities and potentials were expanded inside the muffin-tin spheres in combination with spherical harmonic functions with a cut off lmax = 10, and in Fourier series in the interstitial region. We use a parameter RMT Kmax =8, which determine the matrix size, where RMT denotes the smallest atomic sphere radius and Kmax gives the magnitude of the largest K vector in the plane-wave expansion. All of the calculations were carried out at the theoretical equilibrium lattice constants. We choose the muffin-tin radii of Zn and O to be 0.7 and 2.0 a.u. respectively. The K integration over the Brillouin zone is performed using the Monkhorst– Pack scheme [32] with 1000 K points in the whole Brillouin zone. The self-consistent calculations are considered to be converged only when the calculated total energy of the crystal is converged to less than 0.1 mRyd.

3. Results and discussion

3.1. Structural Properties:

In this section, as a first step, we calculate the phase stability of the binary compound ZnO. The phases considered in this study are zinc blende ZB (B3), NaCl (B1)and wurtzite WZ (B4). To achieve this work, we calculate the total energy as a function of the volume for each compound in the different phases and the obtained curves are fitted to the Murnaghan's equation of state [33]. The results are given in Fig.1. According to these figures, it is found that these compounds adopt the wurtzite B4 structure as a stable phase which is explained by the lowest total energy level. This result is consistent with that of Ustundag et al. [34] using FP-LAPW method. As seen

in these figures, the difference between the minimum energy values of the wurtzite (B4) and zinc blende (B3) phase is small. We can explain this behavior by the bonding mechanism in these structures i.e. The calculated structural parameters such as lattice constants (a and c), c/a ratio, bulk modulus (B), its pressure derivative (B') and equilibrium energy (E0) for the considered structures as well asavailable experimental and theoretical data for the studied compounds are listed in Tables 1 . As shown in these tables, the only results to compare with are those related to zinc-blende, NaCl and wurtzite phases, for the others, the obtained values are predictions and materials. A reasonable agreement is found between our calculated structural parameters and those of literature data.

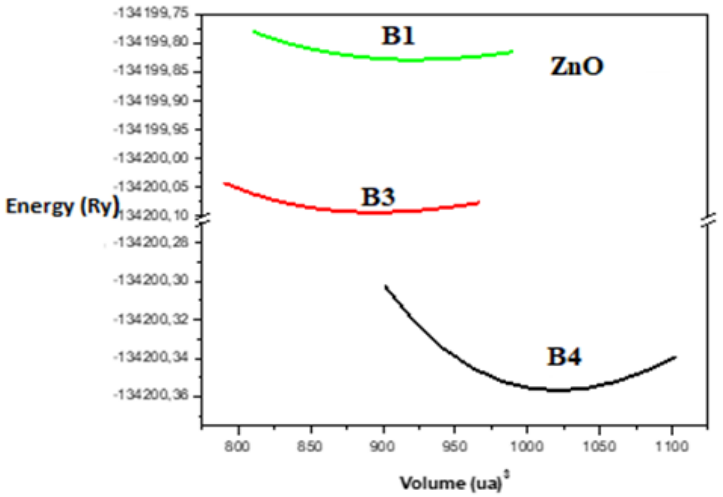

Fig1. Total energy versus volume calculated for ZnO Binary compound.

3.2. Electronic Properties

3.2.1. Band Structure:

We performed a scalar relativistic approximation (without spin-orbit interaction) of the band structure of ZnO at different phases (B1, B3 and B4), using the FP-LAPW method. The band structures are shown in Figure 2. This figure represents the band structures of the ZnO compound in the most stable phase Wurtzite (B4) which belongs to the P63mc symmetry group and the Zinc blende (B3) structure belonging to the symmetry group. F-43m. We used, in the Irreducible Brillouin Zone (IBZ), 63 K points to calculate the band structures. The minimum and maximum of the conduction and valence bands respectively are found at point Γ; therefore we have a direct transition and the dispersion of the bands is similar to the results and findings of other theoretical and experimental work. The energy band gaps (direct and indirect) and valence band widths are listed in Table 1, 2 and 3. From the latter we observe that the lower part of the valence bands is mainly dominated by the (2s) state) of the non-metallic atom (oxygen) with a width equal to 1.155 eV for a maximum dispersion between Γ and M for the most stable phase. Concerning the position in the state (3d) of the cation Zn which is considered localized and influenced by the weight of ten electrons, it is relatively close to the maximum of the valence band derived from the anion (p), and is estimated at 5. 8397 eV; which is largely comparable to the calculations of FPLMTO (-5.1eV) [35], pseudopotential (-5.21eV) [36], GW (-6.4eV) [37]

and the experimental value (-6 .95eV) [38]. On the other hand, in the Rocksalt phase (B1), a structure with a reduced filling rate compared to the Wurtzite ZnO structure presents an indirect gap where the minimum of the conduction band and the maximum of the valence band are located at two different points Γand L. Oxygen atomic states have almost the same contribution as zinc atomic states in the construction of the lower part bands.

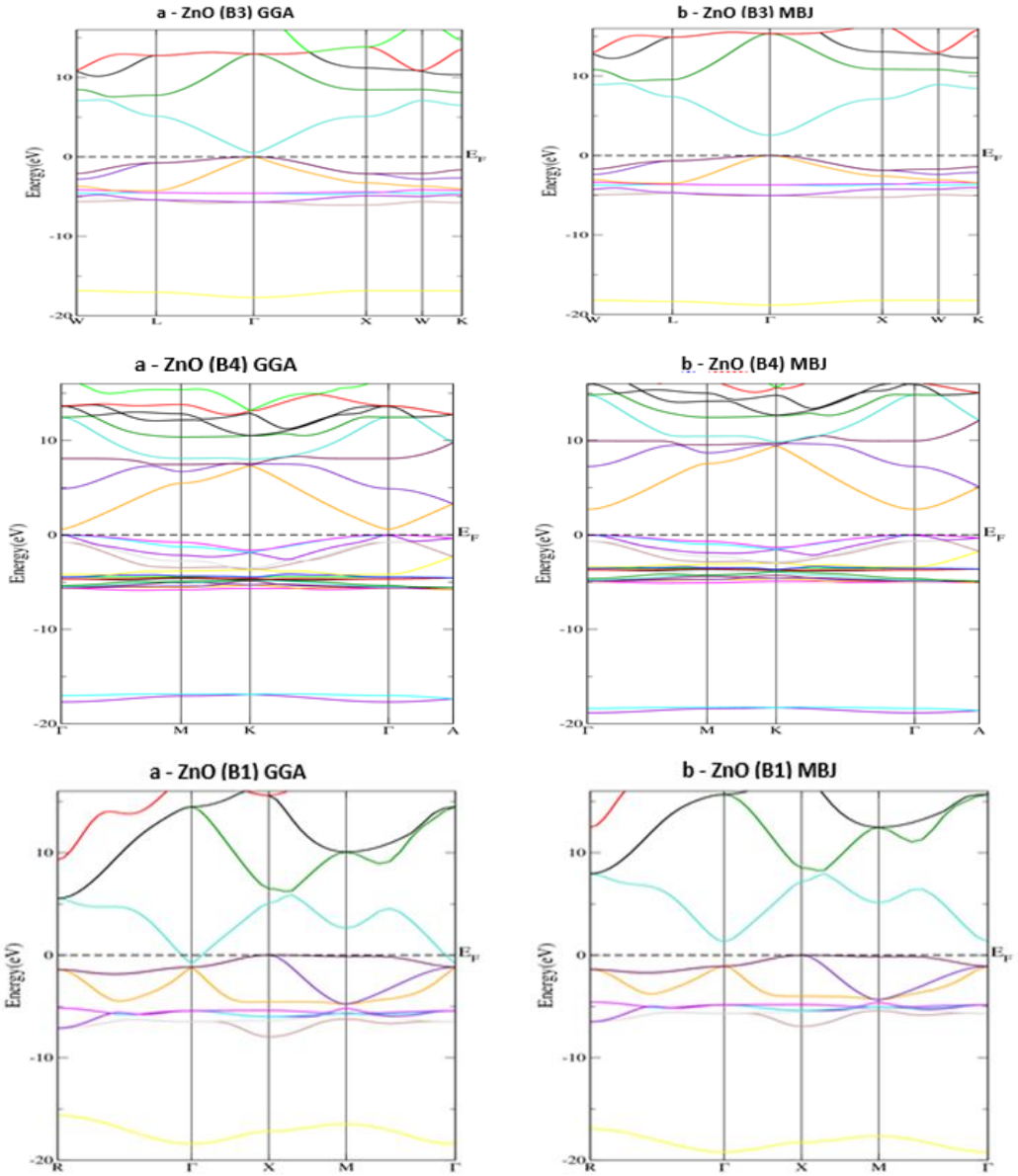

Fig 2: The band structure of ZnOin the Zinc-Blende phase (B3), wurtzite (B4) and NaCl (B1) calculated by: (a) PBE-GGA and (b) mbj.

The following table depicts our ZnO gap values in the three phases (B1, B3 and B4) compared to other theoretical and experimental results. We note that the results we obtained are in agreement with other theoretical results calculated by the same method.

Table 1: Summaries of the different values of the energy gaps and the width of the valence band in the ZnO structure B4.

Phase (B4)			Our results		Theoretical work Other calculations	Exp
			GGA	mbj		
Energy gap (eV):	Direct	(Γ→Γ)	0.8	2.73	0.759[b], 2.683[b], 0.830[b], 2.647[b],0.81[c], 0.80[d], 0.68[e], 0.75[e], 0.76[e], 0.73[e], 0.55[e] ,1.57[f], 0.783[g], 1.80[g]	3.44[i]
		(A→A)	3.63	5.32	3.90[e] ,3.91[d]	
		(M→M)	6.19	8.20	6.73[e], 6.79[d]	
	Indirect	(Γ→A)	3.23	5.03	3.48[e]	
		(Γ→M)	5.45	7.59	1.69[e]	
Band width (eV):		ΔEBV(s)	1.13	0.70		
		ΔEBV(p)	4.19	3.36		
		Valencia-Total Band	17.79	18.82	18.06[e], 18.25[d]	
		Zn-3d(average)	4.4	3.59		
		Gap antisymmetric	10.29	13.93		

Références : b) Réf. [23] c) Réf.[25] d) Réf.[26] e) Réf.[27] f) Réf. [6] g) Réf.[9] i) Réf.[32]

Table. 2: Summaries of the different values of the energy gaps and the width of the valence band in the ZnO structure (B3).

Phase (B1)			Our results		Theoreticalwork Othercalculations	Exp
			GGA	mbj		
Energy gap (eV):	Direct	(Γ→Γ)	2.05	4.06	2.60[c] ,3.07[d]	
		(X→X)	6.64	9.32	7.23[c], 7.74[d]	
		(L →L)	5.46	7.53	5.42[c], 5.43[d]	
		(W→W)	7.29	10.64	9.23[c], 9.57[d]	
		(K→K)	8.72	9.74	7.67[c], 8.00[d]	
	Indirect	(L→ Γ)	0.785	1.21	0.953[b], 1.10[c], 1.31[d], 0.98[e],0.75[f], 1.47[f]	2.45[a]
		(L → X)	4.14	3.42		
Band width (eV):		ΔEBV(s)	1.47	1.07		
		ΔEBV(p)	4.14	3.42		
		Valencia-Total Band	18.18	19.21	18.70[c], 19.23[d]	
		Zn-3d(average)	4.49	4.46		
		Gap	9.67	10.64		

	antisymmetric				

Références :Réf. [23] e) Réf.[27] f) Réf. [28] g) Réf.[28] h) Réf.[31]

Table 3. Summaries of the different values of the energy gaps and the width of the valence band in the ZnO structure (B1).

Phase (B1)			**Our results**		**Theoreticalwork Othercalculations**	**Exp**
			GGA	**mbj**		
Energygap (eV):	**Direct**	**(Γ→Γ)**	**2.05**	**4.06**	**2.60[c] ,3.07[d]**	
		(X→X)	**6.64**	**9.32**	**7.23[c], 7.74[d]**	
		(L →L)	**5.46**	**7.53**	**5.42[c], 5.43[d]**	
		(W→W)	**7.29**	**10.64**	**9.23[c], 9.57[d]**	
		(K→K)	**8.72**	**9.74**	**7.67[c], 8.00[d]**	
	Indirect	**(L→ Γ)**	**0.785**	**1.21**	**0.953[b], 1.10[c], 1.31[d], 0.98[e],0.75[f], 1.47[f]**	**2.45[a]**
		(L → X)	**4.14**	**3.42**		
Band width (eV):		**ΔE_{BV}(s)**	**1.47**	**1.07**		
		ΔE_{BV}(p)	**4.14**	**3.42**		
		Valencia-Total Band	**18.18**	**19.21**	**18.70[c], 19.23[d]**	
		Zn-3d(average)	**4.49**	**4.46**		
		Gap antisymmetric	**9.67**	**10.64**		

Références : a) Réf. [29], b) Réf. [23] c) Réf.[25] d) Réf.[26] e) Réf.[27] f) Réf. [6]

According to figure 2, the compound ZnO belongs to the semiconductor family with direct band gaps; i.e. the electronic transition in the Zinc-blende and the hexagonal structure of the type ((Γ→Γ),), and indirect band gaps with electronic transition in the structure NaCl of the type (L→ Γ))and the structure CsCl of the type (X →Γ). We can seethat the calculated this compound's band gap values—using the GGA and mbj methods coincide more or less with the theoretical results. Furthermore, we also point out that the use of mbj improves the overall band gap values in comparison to those of the GGA.

3.2.2. Total and partial state densities (DOS):

In the LAPW method, the density of states can be decomposed into local partial DOS via:

$$g(E)=g^{out}(E)+\sum_{t,l} g_l^t(E)$$

With being the number of states (electrons)—including Rydberg's spin and the unit cell at energy E which resides in the t sphere and are characterized by spherical harmonics with the

azimuthal quantum number. In the same manner, $g^{out}(E)$ is the number of states (electrons)—including Rydberg's spin and the unit cell at energy E that resides in the interstitial space. The density of states of these compounds is calculated via the Tetrahedron method [15]. The latter requires a substantially large number of special points (273 special points in the Brillouin zone for wurtzite (ZnO) and 84 points for other phases).

A-The Rock salt Phase (B1)

The total DOS and partial PDOS are presented in Figure 3a-b (2D and 3D).

The VB is separated into three parts:

- The first region, which is between -20 eV and -16 eV, consists primarily of the contribution of the O atom (2S) states.
- The second region, between -6 eV and -4 eV,displays a strong contribution from the Zn atom's (3d) orbital whichis dominant close to the maximum valence band, plus a very weak contribution from the O atom (2p) orbital.
- The third region, which ranges from -4 eV to 0 eV, is characterized by contribution from the O atom (2p) orbital anda less strong contribution from and the Zn atom (3d) orbital.

The (CB) conduction bandbottomis predominantly driven by Zn (4s) and O (2p) orbitals.

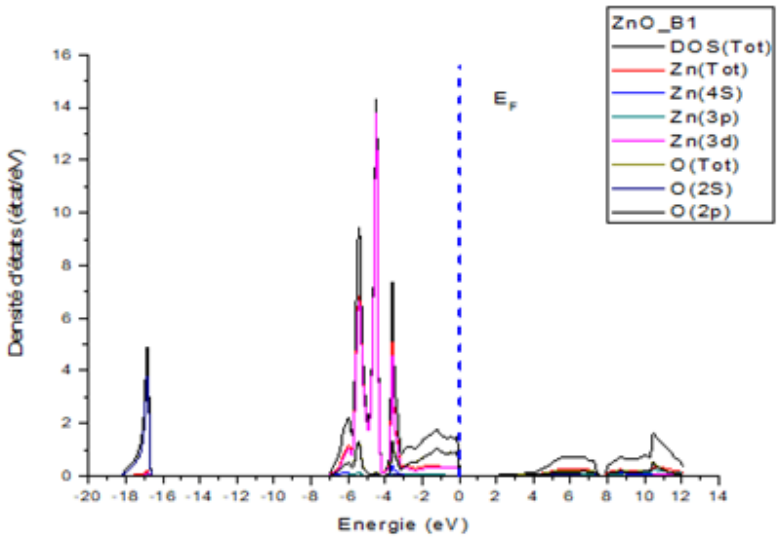

Fig 3.a. .Partial and total state densities of ZnO compound in phase (rock-salt (B1)).

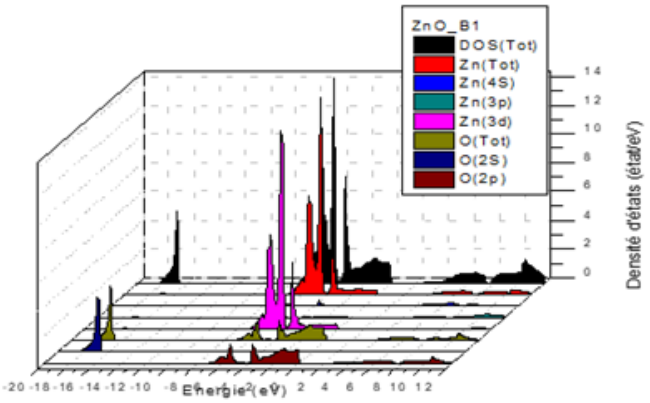

Fig 3.b: Total (DOS) and partial state densities of ZnO in rock-salt phase (B1) (3D)

B-The ZnS Phase (B3):

The total DOS and partial PDOS are presented in Figure 4a-b (2D and 3D).

The VB is separated into three parts:

- The first region, which is between -20 eV and -16 eV, consists primarily of the contribution of the O atom (2S) states.
- The second region, between -6 eV and -4 eV, displays a strong contribution from the Zn atom's (3d) orbital which is dominant close to the maximum valence band, plus a very weak contribution from the O atom (2p) orbital.
- The third region, which ranges from -4 eV to 0 eV, is characterized by contribution from the O atom (2p) orbital and a less strong contribution from and the Zn atom (3d) orbital.

The bottom of the conduction band (BC) is dominated by a mixture of Zn (4s) and O (2p) states.

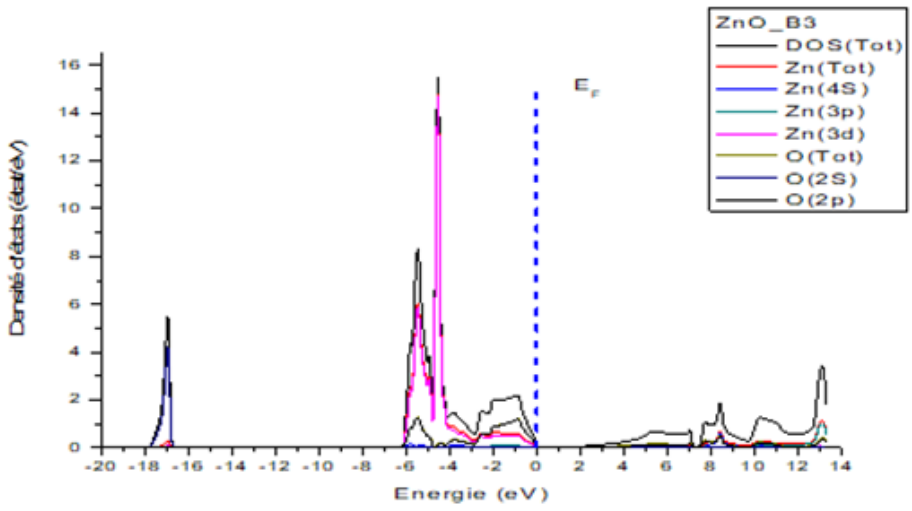

Figure 4 a: Total (DOS) and partial state densities of ZnO in Zinc Blenb (B3) phase.

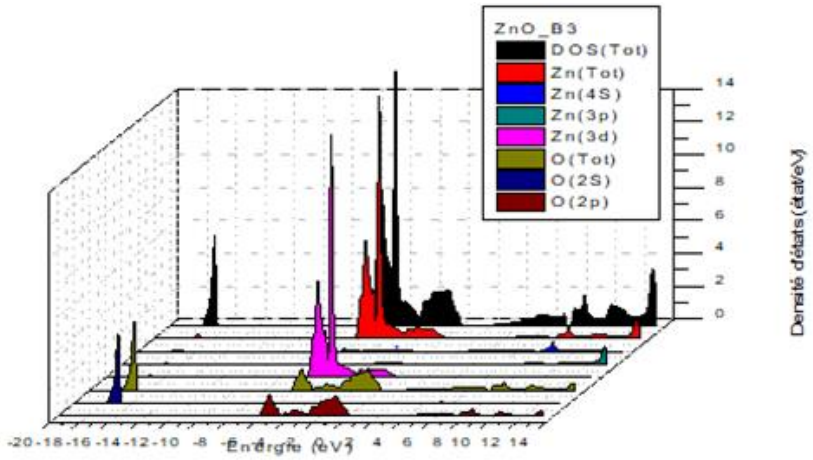

Figure 4. b: Total (DOS) and partial densities of state of ZnO in ZnS (B3) phase (3D).

C-The Wurtzite Phase (B4):

The total DOS and partial PDOS are presented in Figure 5a-b (2D et 3D).

The VB is separated into three regions:

- The first region, which is between -20 eV and -16 eV, consists mainly of the contribution of the O atom (2S) states.
- The second region, between -6 eV and -4 eV, displays a strong contribution from the Zn atom's (3d) orbital which is dominant close to the maximum valence band, plus a very weak contribution from the O atom (2p) orbital.
- The third region, which ranges from -4 eV to 0 eV, is characterized by contribution from the O atom (2p) orbital and a smaller contribution from and the Zn atom (3d) orbital. We also observe a strong hybridization between 3d states of Zn and 2p states of O.

The (CB) conduction band is formed primarily by the Zn Cation 4s states and 2p of the O anion.

The results we obtained via the GGA approximation are in accordance with otherworks cited in the references [39, 40].

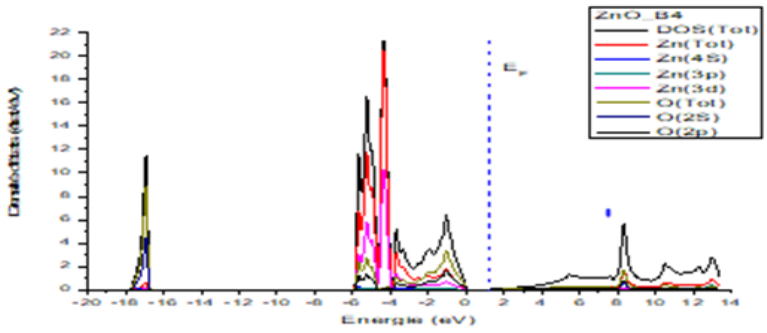

Figure.5.a: Total (DOS) and partial state densities of ZnO in the wurtzite phase (B4).

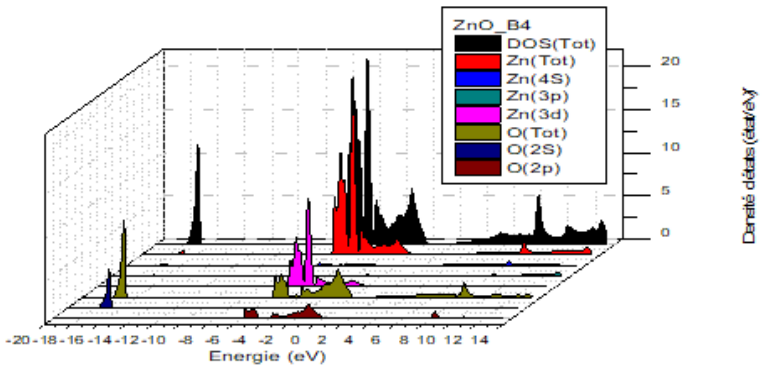

Figure.5. b:Densités d'états totale (DOS) et partielle de ZnOen phase wurtzite (B4) (3D)

3.2.3. Electric Charge Densities: Charge density description is a crucialattribute in the solid because it offers an effective description of chemical properties. The ionic character pertains to charge transfer between cations and anions. Accordingly, using GGA approximation, we calculated ZnO charge densities in the Rocksalt(B1) structure, CsCl(B2), Zincblende(B3), and in the Wurtzite(B4) phase. Charge density results are depicted in the figures (Fig. 6- Fig. 9).

The ionic character occurs when the charge is concentrated around the atomic spheres of atoms and absent in the interstitial spaces. When, on the other hand, the interstitial spaces are full, we have a covalent character.

The element O possesses a higher electronegativity compared to the element Zn as shown in the figures; we notice a transfer of electronic charge from the Zn atom to the O atom.

Charge density in plane 110 of the NaCl structure (B1) indicates a character more ionic than covalent (Fig. 6);that is in agreement with reference [41] which points that the covalent bond is weaker than the ionic bond.

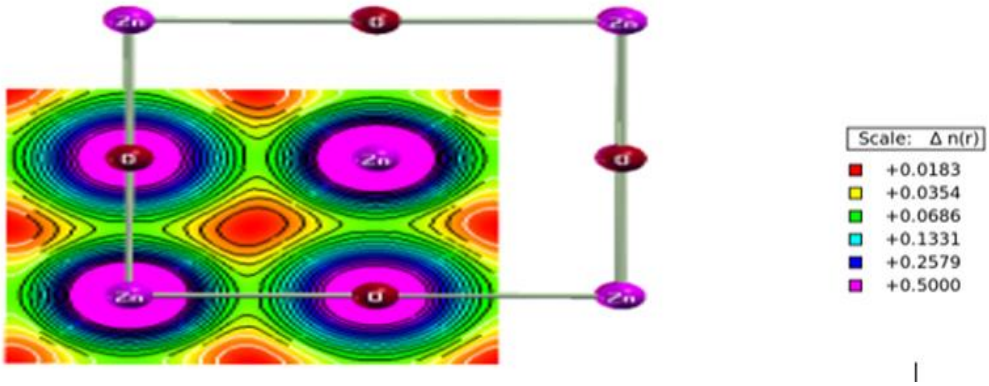

Figure 6: The valence charge density in the (110) plane of ZnO in phase B1.

Charge density in plane 111 of the Zinc-blende phase (B3) is shown in Figure 7 and it indicates a covalent character rather than an ionic character. That corresponds with reference [42].

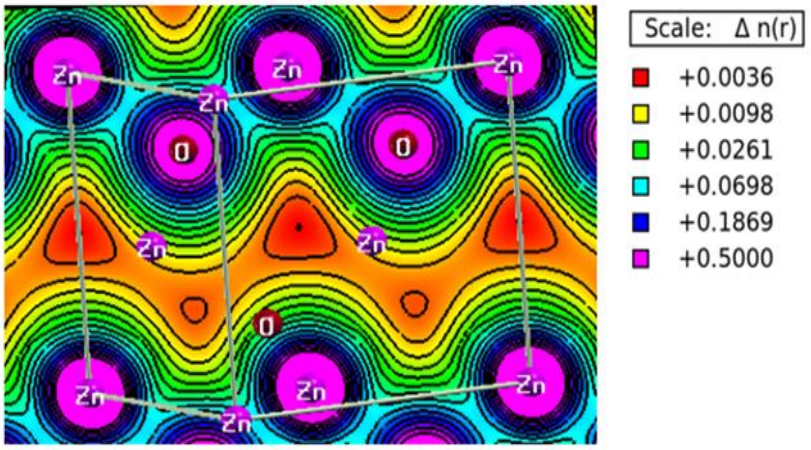

Figure7:Ladensité de charge de valence dans le plan (111) du ZnO dans la phase B3.

Charge density in plane 021 of the Wurtzite phase (B4) is displayedwith details in Figure 8. It equallyindicates a covalent character stronger than the ionic character. The latter is compatible with reference [43] whichindicates an ionic bond that than the covalent bond.

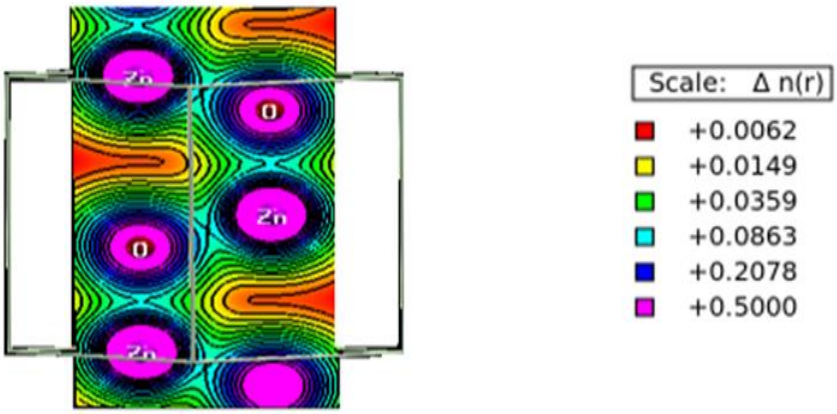

Figure 8: The valence charge density in the (021) plane of ZnO in the B4 phase.

In Tables 4, 5 and 6,, all information on charge transfer is grouped where the difference in charge $Q_{crist}^{Zn} - Q_{at}^{Zn}$ is negative in the Zinc sphere. In the oxygen sphere, the charge of core states (1s2) equals 2. The total crystal charge is represented by core states + 2s 2p 3d nl, and the difference$Q_{crist}^{O} - Q_{at}^{O}$ is positive in all four phases. This indicates that there is more electric charges arounds Oxygen than around Zinc.

Table.4: Analysis of the partial charge of ZnO (B1).

ZnO (B1)	Zn	O
Valencia Charge:		
Inside the spheres		
Atomic		
s	0.33	1.77
p	6.28	4.08
d	9.79	0.02
nl	0.03	0.006
$Q^{in}_{cristal}$total	28.45	7.88
$Q^{in}_{atomique}$ superimposed atomic	28.73	7.50
$Q^{in}_{cristal} - Q^{in}_{atomique}$	-0.28	0.38

Table.5: Analysis of the partial charge of ZnO (B4).

ZnO (B4)	Zn	O
Valencia Charge:		
Inside the spheres		
Atomic		
s	0.34	1.57
p	6.29	3.49
d	9.69	0.012
nl	0.03	0.002
$Q^{in}_{cristal}$total	28.36	7.07
$Q^{in}_{atomique}$ superimposed atomic	28.54	6.85
$Q^{in}_{cristal} - Q^{in}_{atomique}$	-0.18	0.22

Table.6: Analysis of the partial charge of ZnO (B3).

ZnO (B3)	Zn	O
Valencia Charge:		
Inside the spheres		
Atomic		
s	0.34	1.51
p	6.29	3.49
d	9.69	0.012
nl	0.0237	0.0023
$Q^{in}_{cristal}$total	28.34	7.14
$Q^{in}_{atomique}$ superimposed atomic	28.54	6.61
$Q^{in}_{cristal} - Q^{in}_{atomique}$	-0.2	0.53

From these observations we can say that:

There is a charge transfer from the Zinc atom to the nonmetal atom. By analyzing the charge density figures and the corresponding tables, we can observe a high concentration of charge density on the anion side. The latter is characterized by aprominent electronegativity factor compared to the cation side.

4.Conclusion

the study of the structural, electronic and optical properties of the binary compound Zinc Oxide (ZnO). We used in our calculations, an ab-initio method, the linearly augmented plane wave method (FP-LAPW) within the framework of the density functional theory (DFT) implemented in the WIEN2k code. We used the local density approximation (LDA) and the generalized gradient approximation GGA, to perform the calculation of the gaps we used the mBj approximation. Our results of the structural properties are in good agreement with those determined by experiment and other theoretical results obtained by the same method, where the lattice parameters are overestimated by generalized gradient approximations (GGA) and underestimated by local density (LDA).The band structure of our material in the most stable phase presents a direct gap at the point Γ. But, with underestimation of this value because of the use of the GGA approximation, to overcome this problem we used the so-called (mBJ) method which corrects the gap to compare the experimental values. We note that our results are very comparable to the experimental work

References:

[1] Z. X. Xue, Y. Qu, S. L. Ban, Optical phonon limited electron mobility in ZnO nanowires wrapped by MgZnO shells, Journal of Applied Physics, 10.1063/5.0068213, 131, 2, (025104), (2022).
[2] D. C. Langreth and J. P. Perdew, Phys. Rev. B 21, 5469 (1980).
[3] A.Schleife, F. Fuchs, J. Furthmüller, and F. Bechstedt. Phy. Rev. B 73, 245212 (2006)
[4] Murnagham F. D. Proc. Nat. Acad. Sci. USA 30, 244 (1944).
[5] A. S. Mohammadi, S. M. Baizaee and H. salehi.World Applied Sciences Journal 14 (10): 1530-1536, (2011)
[6] Z. Charifi, H. Baaziz, and Ali Hussain Reshak phys. stat. sol. (b) 244, No. 9, 3154–3167 (2007)
[7] A Nancy Anna Anasthasiya, S Ramya, D Balamurugan, P K Rai, B G Jeyaprakash, Adsorption property of volatile molecules on ZnO nanowires: computational and experimental approach, Bulletin of Materials Science, 10.1007/s12034-017-1538-2, 41, 1, (2018).
[8] A.J. Cinthia, G.Sudhapriyanga, procedia Materials Science,5,1034(2014).
[9] H.I.Berrezouga, A.E. Merada, A. Zergab, Z.Sari Hassoun. Energy Procedia 74, 1517 (2015)
[10] Rita John, S. Padmavathi, Crystal Structure Theory and Applications, 5, 24, (2016).
[11] Walter R. L. Lambrecht, Sukit. Limpijumnong, and B. Segall, J. Nitride Semicond. Res. 4S1, G6.8 (1999)
[12] P.Schroer, Krüger, P, et Pollmann, J phys.Rev. B47, 6971 (1993).
[13] Massidda, S., Resta, R., Posternak, M., et Baldereschi, A. Phys.Rev.B52, 16977 (1995).
[14] T. Rezkallah, I. Djabri, M.M. Koç, M. Erkovan, Yu. Chumakov, F. Chemam, Investigation of the electronic and magnetic properties of Mn doped ZnO using the FP-LAPW method, Chinese Journal of Physics, 10.1016/j.cjph.2017.02.021, 55, 4, (1432-1440), (2017).
[15] P. E. Blöchl, O. Jepsen, and O. K. Andersen, Phys. Rev B 49, 16223 (1994).

[16] Darma, Y. Setiawa, F. G, Majidi, M. A., Rusydi, A Adv. Mater. Res. 1112, 41 (2015),
[17] H. Riane, A. Mokaddem, L. Temimi, B. Doumi, S. Bahlouli, F. Hamdache, ZnO/ZnMgO: cubic quantum well laser in UV spectrum, The International Journal of Advanced Manufacturing Technology, 10.1007/s00170-016-9105-3, 89, 1-4, (629-633), (2016).
[18] H.A. Kramers, Nature 117, 775 (1926).
[19] L. Kronig, J. Opt. Soc. Am. 12, 547 (1926).
[20] C. Kittel, « Physique de l'étatsolide ». ed. John Wiley Sons,Inc.7eme ed. (1996).
[21] A. P. Gazhulina, A DFT investigation of 45 wurtzite (B4)-type compounds: Structural, electronic, linear and nonlinear optical properties, International Journal of Modern Physics B, 10.1142/S0217979220500101, (2050010), (2020).
[22] F. Kootstra, P. L. de Boeij, and J. G. Snijders, Phys. Rev. B. 62, 7071 (1999).
[23] Y. Al-Douri, A.J. Haider, A.H. Reshak, A. Bouhemadou, M. Ameri, Structural investigations through cobalt effect on ZnO nanostructures, Optik, 10.1016/j.ijleo.2016.08.012, 127, 20, (10102-10107), (2016).
[24] A. Segura, J.A. Sans, F.J. Manjon, A. Munoz, M.J. Herrera-Cabrera, Appl. Phys. Lett. 83 278(2003).
[25] B.Amran., I.Chiboub, S.Hiadsi,T.Benmessabih, N.Hamdadou. Solid State Commun. 137 (2006) 395–399.
[26] Blaha P, Schwarz K, Madsen GKH, et al. WIEN2K, an augmented plane wave plus local orbitals program for calculating crystal properties. Vienna; 2008.
[27] Hohenberg P, Kohn W. Inhomogeneous electron gas. Phys Rev.;136:864–871(1964)
[28] F.D. Murnaghan, Proc. Natl. Acad. Sci. U. S. A. 30 5390.(1944)
[29] V.L. Shaposhnikov, A.V. Krivosheeva, V.E. Borisenko, J.L. Lazzari, F.A. d'Avitaya, Phys. Rev. B 85 (2012) 20520.
[30] J. S. Toll, Causality and the Dispersion Relation: Logical Foundations, Phys. Rev. 104, 1760 (1956).
[31] L. D. Landau and E. M. Lifshitz, Electrodynamics of Continuous Media (Pergamon Press, Oxford, 1960).
[32] H. A. Kramers, Collected Science Papers (North-Holland Publishing Co, Amsterdam, 1956).
[33] CUI, S, FENG, W, HU, H, Feng, Z et Wang, Y. Journal of Alloys and Compounds, vol. 476, no 1, 306(2009).
[34] Azam Soltani Mohammadi, Seyed. Mahdy Baizaee and Hamdollahsalehi. World Applied Sciences Journal 14 (10): 1530-1536.(2011)
[35] Y.N. Xu, W.Y. Ching, Phys. Rev. B 48 4335.(1993)
[36] A. Segura, J.A. Sans, F.J. Manjon, A. Munoz, M.J. Herrera-Cabrera, Appl. Phys. Lett. 83 278.(2003)
[37] A.Mang, K. Reimann, S. Rubenacke, Solid State Commun. 94 251.(1995)
[38] A.A. Ashrafi, A. Ueta, H. Kumano, I. Suemune, J. Cryst. Growth 221 (2000) 435.
[39] A.Mang, K. Reimann, S. Rubenacke, Solid State Commun. 94, 251 (1995).

[40] H. Ahmoum, M. Boughrara, M.S. Su'ait, M. Kerouad, Effect of position and concentration of Li on ZnO physical properties : Density functional investigation, Chemical Physics Letters, 10.1016/j.cplett.2019.01.032, (2019).

[41] W.N. Shafarman, L. Stolt, in A. Luque, S. Hegedus (Eds.), Handbook of Photovoltaic Science and Engineering, Wiley, Chichester, UK, 2003, pp. 567e616.

[42] J.E. Jaffe, A. Zunger, Phys. Rev. B 29 (1984), 1882; 30 741.(1984)

[43] A.V. Krivosheeva, V.L. Shaposhnikov, F. Arnaudd'Avitaya, V.E. Borisenko, J.- L. Lazzari, J. Phys, Condens. Matter 21 045507. (2009)